Pharm Res (2014) 31:182–193
DOI 10.1007/s11095-013-1151-z

RESEARCH PAPER

Folate-Targeted Nanoparticles Based on Albumin and Albumin/Alginate Mixtures as Controlled Release Systems of Tamoxifen: Synthesis and *In Vitro* Characterization

A. Martínez • R. Olmo • I. Iglesias • J. M. Teijón • M. D. Blanco

Received: 26 February 2013 / Accepted: 16 July 2013 / Published online: 7 August 2013

ABSTRACT

Purpose Preparation and *in vitro* characterization of tamoxifen (TMX)-loaded folate-targeted nanoparticles based on disulfide bond reduced bovine serum albumin (BSA-SH) and BSA-SH/alginate-cysteine (BSA-SH/ALG-CYS) mixtures as drug delivery systems.

Methods Folate-nanoparticles were characterized in terms of folate content, morphology, size, zeta potential, TMX load and drug release kinetics. Additionally, cell viability and cellular uptake of nanoparticles were determined using different cancer cell lines.

Results Folic acid (FOL) was successfully attached to nanoparticles (ranging between 79 and170 μmol folate/g NP). Nanoparticles with 76–417 nm mean size were obtained and loaded with TMX (4.2–7.7 μg/mg NP). Zeta potential and drug extraction revealed major superficial placement of the drug, especially in the case of BSA/ALG-FOL systems. Drug release studies in the presence of surfactant showed a gradual release of the drug between 4–7 h. In general, low cytotoxicity of unloaded systems was found. Internalization of the systems was achieved and mediated by folate receptor, especially in the case of BSA NP-FOL. The administration of 10 μM TMX by TMX-FOL NP showed their efficacy as controlled TMX release systems.

Conclusions Promising anticancer action of these new TMX-loaded folate-targeted systems was demonstrated, allowing a new administration route to be studied in further *in vivo* studies in order to improve current TMX therapy.

Electronic supplementary material The online version of this article (doi:10.1007/s11095-013-1151-z) contains supplementary material, which is available to authorized users.

A. Martínez • I. Iglesias
Departamento de Farmacología, Facultad de Farmacia
Universidad Complutense de Madrid, Madrid, Spain

R. Olmo • J. M. Teijón • M. D. Blanco (✉)
Departamento de Bioquímica y Biología Molecular, Facultad de Medicina
Universidad Complutense de Madrid, Avenida Complutense s/n 28040
Madrid, Spain
e-mail: mdblanco@med.ucm.es

KEY WORDS folic acid · nanoparticles · natural polymers · tamoxifen · targeted therapy

ABBREVIATIONS

ALG-CYS	Alginate-cysteine conjugate
ANOVA	One way analysis of variance
B-50-50 NP	Nanoparticles based on 50% ALG-CYS and 50% BSA-SH
BSA	Bovine serum albumin
BSA-SH	Disulfide bond reduced bovine serum albumin
BSA-SH NP	Nanoparticles based on 100% BSA-SH
C-70-30 NP	Nanoparticles based on 70% ALG-CYS and 30% BSA-SH
DCC	*N*,*N*′-Dicyclohexylcarbodiimide
DMSO	Dimethyl sulphoxide
EDTA	Ethylenediaminetetraacetic acid
FBS	Fetal bovine serum
FOL	Folic acid
KCl	Potassium chloride
MTT	Methylthiazoletetrazolium
NaCl	Sodium chloride
NaOH	Sodium hydroxide
NHS	*N*-Hydroxysuccinimide
NP	Nanoparticles
PBS	Phosphate buffered saline
SDS	Sodium dodecyl sulphate
TMX	Tamoxifen

INTRODUCTION

Recent advances in medicine and health care have significantly improved human life expectancy. Consequently, diseases associated with the elderly, such as cancer, have greatly increased over the past few years. Cancer has been set to become a major cause of morbidity and mortality in coming

decades, the number of new cancer cases being estimated at 20 million by 2013 (1). Thus, there is an increasing need to develop new therapeutic agents, which could be used either singly or combined with conventional therapies, and which would cause less toxicity and provide a better quality of life to patients.

Nanomedicine is the branch of nanotechnology that applies the emerging properties of materials on a nanoscale to achieve faster diagnosis, improved imaging, enhanced therapeutics and prevention of various clinical conditions (2). The technology has been especially focused in cancer treatment and diagnosis to overcome the lack of specificity and resistance developed to conventional chemotherapeutic agents (3).

Nanoparticle-based drug-delivery systems have made a remarkable difference to controlled drug delivery of chemotherapeutic agents during the last two decades. Their physical, biological and chemical attributes play an important role in their intracellular uptake, high loading capacity and specific targeting to tumour cells (4). However, only a selected number of these new nanoparticulated systems have been released to the market, whichare routinely used in clinics (5), such as Abraxane™ (albumin-paclitaxel nanoparticles) or Nanoxel™ (N-isopropyl acrylamide paclitaxel embebbed micelles).

Due to their small size, nanoparticles are capable of taking advantage of the leaky vasculature and poor lymphatic drainage system of tumours to enhance the retention time of packed drugs (passive targeting) by a factor of 10 (6). However, a new and promising strategy is being developed using biological ligands covalently attached to nanoparticles which can be selectively recognized by tumour cells (active targeting). That leads to a reduction in the minimum effective dose of the drug and its toxicity, while also improving its therapeutic efficacy (7). Among the several molecules that have been identified as possible ligands for coupling to nanoparticulated systems, folic acid has been one of the most commonly used since folate receptor (FR) over expression has been identified in a wide range of tumours, such as in ovarian, endometrial, colorectal or breast cancer (8). Some recent works have shown the enhanced uptake of folate-conjugated nanoparticles based on natural polymers by cancer cells (9,10) These systems combine the advantages of biocompatibility and biodegradability which natural polymers offer with the enhanced uptake of the systems mediated by folate-targeting.

Proteins and polysaccharides have been widely used separately as biopolymers to develop new drug delivery systems. However, the combination of both types of polymers offers new possibilities and better functional properties that that of each molecule alone (11). Several properties of protein-polysaccharide complexes, such as solubility, viscosity, aggregation or gelation, allow their application into different fields. Moreover, some of these properties can be modulated by controlling pH, biopolymer ratio and weight, temperature or ionic strength, which make them very versatile complexes with different applications.

Alginate/BSA nanoparticles prepared by an emulsion method have been previously used for the controlled delivery of anticancer drugs, such as 5-fluoruracil (12). However, the combination of disulfide bond reduced albumin and thiolated alginate offers all the advantages of protein/polysaccharide complexes, and also the possibility of stabilizing particles though disulfide bond formation. This is a simple process that is totally carried out in aqueous medium, and it can be induced by changing pH conditions. Additionally, disulfide bonds are present in biological environment, which contributes to the aim of biocompatibility and biodegradability of these systems.

In this study, folate-targeted nanoparticles based on disulfide bond reduced bovine serum albumin (BSA-SH) and BSA-SH/alginate-cysteine conjugate (ALG-CYS) mixtures have been prepared and loaded with tamoxifen (TMX), a selective oestrogen receptor modulator widely used in breast cancer treatment (13). They were also *in vitro* characterized *in vitro* in order to evaluate their application in targeted tumour therapy.

MATERIALS AND METHODS

Materials

Alginic acid sodium salt (viscosity 200.000–400.000 cps), folic acid, *N*-Hydroxysuccinimide (NHS), *N,N*-Dicyclohexylcarbodiimide (DCC), trypsin from bovine pancreas (13,000 units/ mg solid), gentamicin (50 μg/mL), dimethyl sulphoxide (DMSO), methylthiazoletetrazolium (MTT), Coumarin 6 and tamoxifen (TMX) were purchased from Sigma-Aldrich (Barcelona, Spain). Sodium hydroxide (NaOH), hydrochloric acid (HCl; 35%), ethanol absolute, triethylamine, methanol (HPLC gradient grade), ethylenediaminetetraacetic acid (EDTA), potassium chloride (KCl) and potassium di-hydrogenphosphate were purchased from Panreac (Barcelona, Spain). Bovine serum albumin (BSA, Fraction V), sodium chloride (NaCl), di-sodium hydrogenphosphate dihydrated and sodium dodecyl sulphate (SDS) were purchased from Merck (Barcelona, Spain). Fetal bovine serum (FBS), penicillin (50 U/mL), streptomycin (50 μg/mL), L-glutamine (200 mM) and 0.05% trypsin/0.53 mM EDTA were purchased from Invitrogen Life Technologies (Grand Island, NY, USA). Dulbecco's modified Eagle medium was purchased from Lonza (Belgium).

Methods

Preparation of Nanoparticles

Nanoparticles of disulfide bond reduced bovine serum albumin (BSA-SH) and BSA-SH/alginate-cysteine conjugate

(ALG-CYS) mixtures were prepared according to the methodology developed in previous studies (14,15). Briefly, an aqueous solution of BSA 5% (w/v) was treated with 2-mercaptoethanol in order to obtain BSA-SH, and ALG-CYS conjugate was synthesised by attaching L-cysteine molecules to alginate backbone by a carbodiimide-mediated reaction (15). Then, a determined amount of BSA-SH and ALG-CYS was dissolved in 20 ml 1 mM HCl with vigorous stirring. The suspension obtained was sonicated (Branson sonifier 450) and, in order to oxidize free thiol groups and form disulfide bonds, pH was adjusted to 6.5–6.8 with 1 M NaOH (16). The reaction was allowed to proceed for 12 h under intense stirring conditions. Then, 5 ml of a solution of L-cysteine (0.06 mM) was added and the reaction was maintained for a further 5 h with vigorous stirring to block any free thiol groups possibly remaining. After this time the resulting suspension was centrifuged (41,000 rpm, 15 min, Beckman Coulter Optima L-100 XP Ultracentrifuge), and nanoparticles were freeze dried for 24 h at −110°C. Nanoparticles with50% ALG-CYS and 50% BSA-SH (v/v, B-50-50 nanoparticles), 70% ALG-CYS and 30% BSA-SH (v/v, C-70-30 nanoparticles), and 100% BSA-SH (v/v, BSA-SH nanoparticles) were prepared. The final BSA-SH/ALG-CYS ratio in nanoparticle composition was 1.16/1 and 0.49/1 in the case of B-50-50 and C-70-30 nanoparticles, respectively, as previous studies indicated (15). Nanoparticles with the three compositions were prepared and selected to be conjugated with folic acid.

Preparation of Folate-Conjugated Nanoparticles

The *N*-Hydroxysuccinimide ester of folic acid (NHS-folate) was prepared according to the method developed by Lee and Low (17). Folic acid (2.5 g) was dissolved in 50 ml of dry dimethyl sulfoxide (DMSO) plus 1.25 ml of triethylamine, and reacted with *N*-hydroxysuccinimide (NHS) (1.3 g) in the presence of dicyclohexylcarbodiimide (2.35 g) overnight at room temperature. The by-product, dicyclohexylurea, was removed by filtration. The DMSO solution was then freeze-dried, and NHS-folate was precipitated in diethylether. The final product, NHS-folate, was washed several times with anhydrous ether, dried under vacuum, and yielded a yellow powder.

The conjugation of folate to nanoparticles was carried out following the method developed by Zhang and co-workers (18): NHS-folate (50 mg) was dissolved in 1.0 mlDMSO and added slowly to 2 ml of the stirried nanoparticle suspension (10 mg NP/ml, pH adjusted to 10 using 1 M carbonate/bicarbonate buffer). After stirring for 45 min at room temperature, the reaction mixture was centrifuged and washed (41,000 rpm, 20 min) in order to separate the folate-conjugated nanoparticles from unreacted folic acid and other by-products. Finally, folate-conjugated nanoparticles (B-50-50-FOL, C-70-30-FOL and BSA-SH-FOL NP), were freeze dried for 24 h at −110°C.

Determination of Folate Content

The amount of folate conjugated to albumin amine groups was determined by spectrophotometric analysis (18). 2 mg folate-conjugated nanoparticles were hydrolysed by trypsin (0.05 mg/mg NP) with stirring at 37°C for 2 h. After the digestion process, the quantification of folate-conjugation was performed by spectrophotometric measurement of its absorbance at 358 nm (folic acid $\varepsilon = 8643.5\ M^{-1}\ cm^{-1}$).

Preparation of TMX-Folate-Conjugated Nanoparticles

TMX loading into folate-conjugated nanoparticles was based on the methodology used in previous studies (14). Briefly, after folate-conjugated nanoparticles were obtained, 20 mg of nanoparticles were suspended in 1 ml of a 500 μg/ml TMX solution (in ethanol) and incubated for 12 h at room temperature. Finally, the suspension was centrifuged (41,000 rpm, 15 min) and the nanoparticles were again freeze-dried. All the experiments with TMX were performed under subdued light as the drug is highly photosensitive.

Morphology, Size and Zeta Potential Measurements

The appearance and size of folate-conjugated nanoparticles were studied by scanning electron microscopy (FE-SEM) (Jeol JSM-6400 Electron Microscope, resolution 3.5 nm from Centro de Microscopía y Citometría, UCM). Size and zeta potential measurements of TMX-loaded and unloaded systems were performed in deionized distilled water using a back-scattered quasi-elastic light scattering device (Zetatrac NPA-152, Microtrac). Data was processed with Microtrac Flex Software.

Estimation of Drug Content

In order to determine the amount of TMX loaded into folate-conjugated nanoparticles, an enzymatic digestion of TMX-loaded folate-conjugated nanoparticles was carried out based on the methodology developed in previous works (14). Briefly, 2 mg of TMX-loaded nanoparticles were suspended in 2 ml of phosphate buffered saline (PBS, pH = 7.4) and 100 μg trypsin were added to the solution. The digestion process was performed under stirring at 37°C for 24 h. After this time, TMX was extracted from PBS solution by the addition of 4 ml of dichloromethane. The tubes were mixed in a vortex mixer for 10 min and then centrifuged for 20 min at 3,000 rpm. The organic phase was transferred to vials and evaporated to dryness. The resulting residue was reconstituted in methanol and then evaluated by HPLC. In order to establish the efficacy

of the extraction process, 2 mg of unloaded nanoparticles were suspended with a known concentration of TMX in PBS and 100 μg of trypsin, and the same extraction protocol was followed.

A direct extraction of the drug from TMX-loaded nanoparticles was carried out using methanol in order to study the strength of the interaction between the drug and the system (14,15): 3 mg of TMX-loaded nanoparticles were suspended in 1 ml of methanol with stirring for 5 h. After this time, the suspension was centrifuged (13,000 rpm, 5 min) and the supernatant liquid was collected for measurement. The samples obtained in all processes were analyzed by HPLC.

High Performance Liquid Chromatography (HPLC) with a fluorescence detector was required to determine the drug content (19,20). The chromatographic separation was performed on a 25 cm × 4.6 mm RP-Spherisorb ODS2 C_{18} column (5 μm particle size, Waters). The mobile phase consisted of 1% aqueous solution of triethylamine and methanol 11/89 (v/v). A flow rate of 1 ml/min was established. The fluorescence detector was set at an excitation wavelength of 250 nm and an emission wavelength of 370 nm. A photochemical reactor unit with a wavelength of 254 nm was placed between the detector and the column. Chromquest 4.2 software (Thermo) was used to process the data obtained. The limit of detection of TMX established by this method was 1 ng/ml. Standard solutions (10–2,000 ng/ml) of TMX in methanol were used to obtain the calibration curve and a good linear correlation ($r^2 = 0.99$) was obtained.

Drug Release Studies

For drug release studies from TMX-loaded folate-conjugated nanoparticles, 5 mg of drug-loaded nanoparticles was added to 5 ml PBS (pH = 7.4) with 0.5% SDS contained in a flask vial at a constant temperature (37°C) and at orbital shaking (100 rpm, Ecotron INFORS HT). TMX is relatively insoluble in the aqueous medium and SDS is an anionic surfactant used to make the release of the drug easier in phosphate buffer (21). At intervals, 50 μL samples were withdrawn from the solution in order to follow the change in drug concentration using HPLC. The volume removed from the vial was replaced with PBS with 0.5% SDS. Additionally, a parallel drug release study was performed in PBS (pH = 7.4) without SDS to compare the amount of drug released at 24 h under more physiological conditions with TMX released in the presence of SDS. Sink conditions were maintained during drug release experiments (22).

In Vitro Cell Culture Studies

Cell Culture. Human breast adenocarcinoma MCF-7 and T47D cells were obtained from Dr. von Kobbe and Dr. Pérez-Castillo, respectively, and human cervical cancer HeLa cells were obtained from Dr. Tierrez, whose original source was ATCC® and between 20 and 25 passage numbers. Cells were maintained in Dulbecco's modified Eagle medium, supplemented with 10% heat inactivated FBS, penicillin (50 U/mL), streptomycin (50 μg/mL), L-glutamine (200 mM) and gentamicin (50 μg/mL) in a humidified incubator at 37°C and 5% CO_2 atmosphere (HERA cell, Sorvall Heraeus, Kendro Laboratory Products Gmbh, Hanau, Germany). Cells were plated in 75-cm^2 flask (Sarstedt Ag and Co., Barcelona, Spain) and were passaged when reaching 95% confluence, by gentle trypsinization.

Immunofluorescence Analysis. The expression of FR-α in MCF-7, T47D and HeLa cell lines was determined and quantified by the immunofluorescence technique (23) using a specific monoclonal murine antibody (MAb Mov18/ZEL, Enzo Life Sciences, Switzerland) (24). Cells were seeded in 24-well flat-bottom plates at 50,000 cells per well for MCF-7 and T47D, and 25,000 cells per well for HeLa. Twenty-four hours later, cells were harvested and washed with fluorescence-activated cell sorting (FACS) buffer (PBS containing 0.1% sodium azide and 5% FBS). Approximately, 10^6 cells were then suspended in 200 μl of FACS buffer with saturating concentrations (10 μg/ml) of the primary anti FR-α MOv18 or isotypic control IgG murine antibody Biolegend, Germany). After incubation on ice for 1 h, the cells were washed twice in FACS buffer, and incubated for an additional 30 min at 4°C with optimal dilutions of goat anti-mouse-IgG Alexa488-conjugated second step antibody (Enzo Life Sciences, Switzerland). At the end of the incubation, the cells were washed 3 times with PBS at 4°C and fixed in 1% buffered paraformaldehyde. Samples were analyzed with a FACScan flow cytometer using CellQuest software (BD Biosciences, Mountain View, CA). Cells were analyzed by gating based on forward and side scatter. Results are expressed as fluorescence index (FI) defined as FR-α associated fluorescence divided by isotypic control fluorescence.

Cellular Uptake of Nanoparticles. Cellular uptake of folate-conjugated nanoparticles and non folate-conjugated nanoparticles was investigated with a monoculture of MCF-7, T47D and HeLa cells using the methodology developed in previous works (14). Briefly, nanoparticles were loaded with Coumarin following the protocol previously used (14). Cells were seeded in 96-well flat-bottom plates at 10,000 cells per well for MCF-7 and T47D cells and at 5,000 cells per well for HeLa. Twenty-four hours later, the medium was replaced with 100 μl medium with 1% FBS containing 1 mg of Coumarin-loaded folate-targeted and non-targeted nanoparticles per ml of growth medium. The plates were incubated at 37°C for 2 and 24 h. Then, the cells were washed thoroughly with PBS in order to remove the nanoparticles which had not been effectively internalized by the cells. Finally, MCF-7, T47D and HeLa cells were dried overnight and

dissolved in 100 µl of lysis reagent (PBS with 2% SDS and 50 mM EDTA). Remaining nanoparticles were quantified by fluorimetry at 488 nm using a spectrophotometer (Varioskan, Thermo Fisher Scientific, Barcelona, Spain). In order to calculate the amount of nanoparticles from fluorescence, calibration curves (fluorescence *versus* concentration) were prepared in the same lysis medium.

For a competitive binding assay (25), folate receptors were blocked with incubation medium including 1 mM free folic acid 2 h before adding nanoparticles. Then, the medium was replaced with nanoparticles suspended in medium +1 mM free folic. Plates were incubated at 37°C for 2 h and, after this time, the same protocol as previously described was followed.

Additionally, microscopy studies were carried out before removing PBS from the final wash. Localization of fluorescent dye was examined by light fluorescence microscopy (Leica DMIL microscope, Leica Microsystems Switzerland). Cells were photographed with a Leica DFC 300FX digital camera and Leica Application Suite software was used for processing the pictures (Leica Microsystems Switzerland). This experiment was carried out only with those systems that showed an enhanced uptake when they were functionalized with folate (B-50-50-FOL and BSA-SH-FOL NP), taking into account the results obtained in the uptake assay previously described.

Cell Viability. Cell viability was evaluated by using the MTT method. All experimental conditions were performed in quintuplicate. Each experiment was carried out in triplicate. 10 µM TMX was used, having been determined as the most effective concentration in preliminary experiments (14). Cells were seeded in 96-well flat-bottom plates at 5,000 cells/well, in the case of MCF-7 and T47D cells, and at 2,500 cells/well, in the case of HeLa cells. After 24 h, the medium was replaced with 100 µl medium with 1% FBS containing unloaded folate-conjugated nanoparticles, TMX-loaded folate-conjugated nanoparticles or the drug in solution. The amount of nanoparticles was 0.929 mg/mL in the case of B-50-50-FOL and BSA-SH-FOL NP, and 0.620 mg/ml for C-70-30-FOL NP which was in accordance with the concentration of TMX considering the TMX load of the particles. Medium was not removed or changed up to 1, 2, 3, 6 and 9 days, when 10 µl MTT solution (5 mg/ml) was added to each well. After 2 h incubation at 37°C, 5% CO_2, each well was replaced with 100 µl DMSO (26). Cell viability was determined by measuring the absorbance at 570 nm using a spectrophotometer (Varioskan, Thermo Fisher Scientific, Barcelona, Spain). Results are presented as the percentage survival in relation to untreated control cells.

Statistical Analysis

Statistical comparisons were performed using one way analysis of variance (ANOVA) following by Bonferroni post hoc analysis with computer software SPSS 19.0. Values of $p<0.05$ and $p<0.01$ were considered significant and very significant, respectively.

RESULTS

Determination of Folate Content

A spectrophotometric measurement was carried out after the tryptic hydrolysis of nanoparticles to evaluate the extent of folate-conjugation in folate-conjugated nanoparticles. 170±13, 143±25 and 79±29 µmol folate/g NP were determined for BSA-SH-FOL, B-50-50-FOL and C-70-30-FOL NP, respectively. The amount of folate conjugated to C-70-30-FOL NP was significantly lower ($p<0.05$) than that bound to BSA-SH-FOL and B-50-50-FOL NP.

Morphology, Size and Zeta Potential Measurements

Morphology of BSA-SH-FOL, B-50-50-FOL and C-70-30-FOL NP was analysed by FE-SEM. FE-SEM micrographs of nanoparticles (Fig. 1) showed individual nanometric particles, with certain spherical tendency, and apparently non porous and smooth surface.

Each nanoparticle formulation was also analysed using quasi-elastic light scattering in order to characterize TMX-loaded and unloaded folate-conjugated nanoparticles in terms of mean size and surface charge. All nanoparticles showed nanometric size. BSA-SH-FOL, B-50-50-FOL and C-70-30-FOL NP unloaded systems showed mean diameter of 350, 68 and 98 nm, respectively (Fig. S1; Supplementary Material). TMX-BSA-SH-FOL, TMX-B-50-50-FOL and TMX-C-70-30-FOL nanoparticles showed mean diameter of 417, 76 and 104 nm, respectively (Fig. S1; Supplementary Material).

Zeta potential analysis revealed that BSA-SH-FOL, B-50-50-FOL and C-70-30-FOL NP unloaded systems had zeta potential values of −10±4, −23.4±0.6 and −43±3 mV, respectively. In the case of TMX-loaded systems, TMX-BSA-SH-FOL, TMX-B-50-50-FOL and TMX-C-70-30-FOL nanoparticles showed zeta potential values of 5±2, 42±2 and 32±6 mV, respectively.

Estimation of Drug Content in Nanoparticles

An enzymatic degradation was carried out in order to quantify the TMX load of the folate-conjugated systems. TMX-BSA-SH-FOL, TMX-B-50-50-FOL and TMX-C-70-30-FOL nanoparticles showed values of 4.9±0.5, 4.2±0.3 and 7.7±0.8 µg TMX per mg nanoparticle, respectively. According to these results, TMX-C-70-30-FOL nanoparticles included significantly ($p<0.01$) more drug than TMX-B-50-

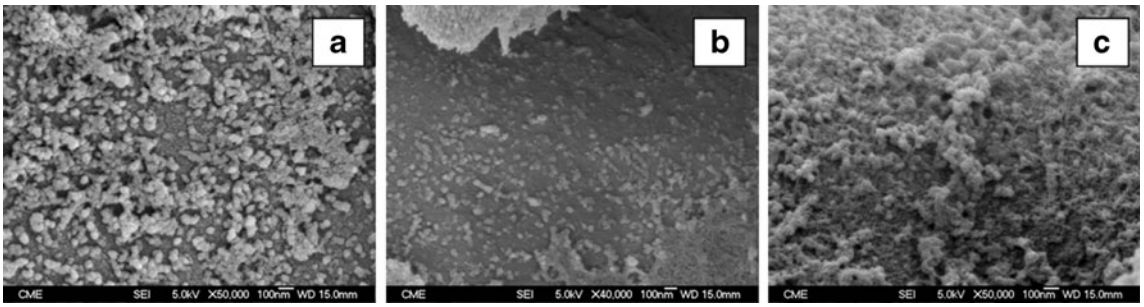

Fig. 1 FE-SEM micrographs of nanoparticles: BSA-SH-FOL NP (**a**), B-50-50-FOL NP (**b**) and C-70-30-FOL NP (**c**).

50-FOL and TMX-BSA-SH-FOL nanoparticles, which showed similar values.

In the case of TMX extraction with methanol, TMX-BSA-SH-FOL, TMX-B-50-50-FOL and TMX-C-70-30-FOL nanoparticles showed values of 1.9±0.3, 4.1±0.5 and 6.1±0.7 μg TMX per mg nanoparticle, respectively. Thus, this method allowed the complete extraction of the drug to be achieved in the case of nanoparticles with alginate in their composition, but only 38% of the average drug load value was extracted in the case of albumin nanoparticles.

Drug Release Studies

The cumulative release curve of TMX in the presence of SDS in the release medium is represented in Fig. 2. Maximum drug release obtained from each formulation is shown in Table I. TMX release was complete in all cases, since differences between maximum drug release values and TMX load of nanoparticles determined by enzymatic degradation were not found to be statistically significant ($p > 0.05$).

Drug release in the presence of SDS occurred rapidly for the first 3 h, 2 h and 1.5 h, when 39%, 36% and 62% of TMX was released from TMX-BSA-SH-FOL, TMX-B-50-50-FOL and TMX-C-70-30-FOL, respectively. From this point onward, a slower second stage was established and the TMX release rate could be determined. These values are shown in Table I.

Additionally, the amount of TMX released from the systems was quantified at 24 h in a parallel study performed in the absence of SDS. 0.2±0.1, 0.12±0.03 and 0.18±0.03 μg TMX/mg NP values were determined for TMX-BSA-SH-FOL, TMX-B-50-50-FOL and TMX-C-70-30-FOL, respectively. These data were significantly different ($p < 0.01$) from the respective values at 24 h in the presence of SDS in the release medium (3.99±0.08, 4.8±0.2 and 5.8±0.4 μg TMX/mg NP in the case of TMX-BSA-SH-FOL, TMX-B-50-50-FOL and TMX-C-70-30-FOL, respectively).

In Vitro Cell Culture Studies

Three different cellular lines, MCF-7, T47D and HeLa cells, were selected according to their expression of estrogen receptor (ER) and folate receptor (FR) to assay the nanoparticles and evaluate, not only the antiestrogenic action of the drug, but also the uptake of the systems mediated by the FR.

Immunofluorescence analysis was employed to quantify the expression of FR-α on MCF-7, T47D and HeLa cell surface using a specific monoclonal antibody. Figure 3 shows the histogram of associated FR-α fluorescence of the three cell lines. As can be observed, the receptor presence was confirmed in all the lines, but not in the same proportion. Very similar FR-α expression was observed in the case of MCF-7 and T47D cells, the MCF-7 cell line being slightly more FR-α expressive than T47D cells (8.9 and 7.7, respectively). HeLa cells were the most FR-α expressive and showed the highest FI value (24.9).

Folate-conjugated nanoparticles and non folate-conjugated nanoparticles were loaded with a fluorescent marker and added

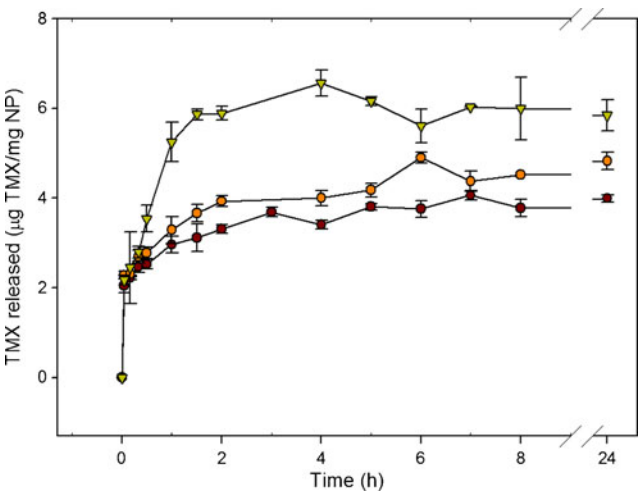

Fig. 2 Cumulative amount of TMX released from drug-loaded TMX-BSA-SH-FOL NP (—●—), TMX-B-50-50-FOL NP (—●—) and TMX-C-70-30 NP-FOL (—▼—).

Table I Maximum Drug Release and Release Rates of Tamoxifen from Nanoparticle Formulations

Sample	Maximum drug release (μg TMX/mg NP)	Time	Release rate in second stage K (μg TMX/mg NP/h)[a]	Second stage time interval
TMX-BSA-SH-FOL	4.1 ± 0.1	7 h	0.018 (0.932)[a]	3–8 h
TMX-B-50-50-FOL	4.9 ± 0.1	6 h	0.124 (0.989)[a]	4–8 h
TMX-C-70-30-FOL	6.6 ± 0.3	4 h	0.023(0.905)[a]	1.5–8 h

[a] Value in parenthesis is r^2

to cells in order to study their cellular uptake. Fluorescent signal into cells was quantitatively and qualitatively detected after 2 and 24 h of incubation. Results are shown in Fig. 4. As can be observed, either targeted or not targeted systems were internalized. However, B-50-50-FOL and BSA-SH-FOL NP enhanced their uptake when the systems were functionalized with folate while no differences were found in the case of C-70-30-FOL NP. B-50-50-FOL was highly internalized by the three lines, and BSA-SH-FOL uptake was especially relevant in case of HeLa cells.

Besides the quantitative assay, the internalization of these systems was easily observed due to the green fluorescence of coumarin attached to the particles, as shown by the images obtained from the fluorescence microscope (Fig. 4).

A competitive binding assay was carried out at 2 h to assess if FR was responsible for the increased uptake of B-50-50-FOL and BSA-SH-FOL NP by adding free folic acid to the incubation medium. FR seemed to be mainly involved in BSA-SH NP uptake by the three cell lines and in B-50-50-FOL NP uptake by T47D cells, as nanoparticle uptake values significantly decreased when free folic acid was added to the medium (Fig. 4). However, B-50-50-FOL NP uptake by MCF-7 and HeLa cells could not be exclusively attributed to FR, since uptake reduction in the presence of free folic acid was not found to be statistically significant (Fig. 4).

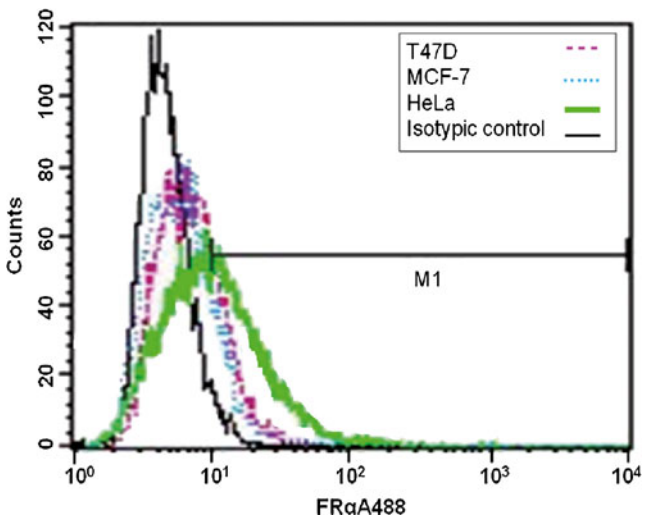

Fig. 3 Histogram with associated FR-α fluorescence of MCF-7, HeLa and T47D cells.

Cytotoxicity studies were carried out over 1, 2, 3, 6 and 9 days with unloaded folate-conjugate nanoparticles using the equivalent concentration to 10 μM TMX when drug was administered by nanoparticles in later studies. In the case of MCF-7 cells, B-50-50-FOL and C-70-30-FOL NP generally caused low cytotoxicity (cell survival between 99±8% and 73±8%), and showed the lowest viability values after 9 days of incubation. However, BSA-SH-FOL caused a significant decrease in cell viability from the first day of incubation (between 69±4% and 57±8%). In the case of HeLa cells, cell survival was significantly reduced with B-50-50-FOL and BSA-SH-FOL NP from the third day of incubation (between 68±5% and 50±12%). For C-70-30-FOL NP, low toxicity was observed during the first three days of incubation (between 108±9% and 71±8%) but this value decreased to 44±8% at day 9. Finally, in the case of T47D cells, a similar situation was observed to that of MCF-7 cells. B-50-50-FOL and C-70-30-FOL NP caused low cytotoxicity over the complete study (between 105±10% and 78±11%) and showed the lowest values after 9 days of incubation. BSA-SH-FOL caused a significant decrease in cell viability from the first day of incubation (between 73±16% and 62±7%).

Finally, 10 μM TMX was administered to cells in solution and entrapped into nanoparticles to check the efficacy on gradual reduction of cell survival at 1, 2, 3, 6 and 9 days (Fig. 5). TMX administered entrapped into folate-systems caused more gradual decrease in cell viability than when TMX was administered in solution from the first day, in the case of HeLa and T47D cells, and from the third day, in the case of MCF-7.

DISCUSSION

Current TMX therapy for advanced or metastatic oestrogen-dependent breast cancer has been associated with some serious side effects after long-term treatment. Thus, research on new challenging targeted therapies has become a necessity. Folate receptor plays a significant role in a wide range of tumour types, including breast cancer (7). It has been hypothesized that folate-attached therapeutic agents might reduce

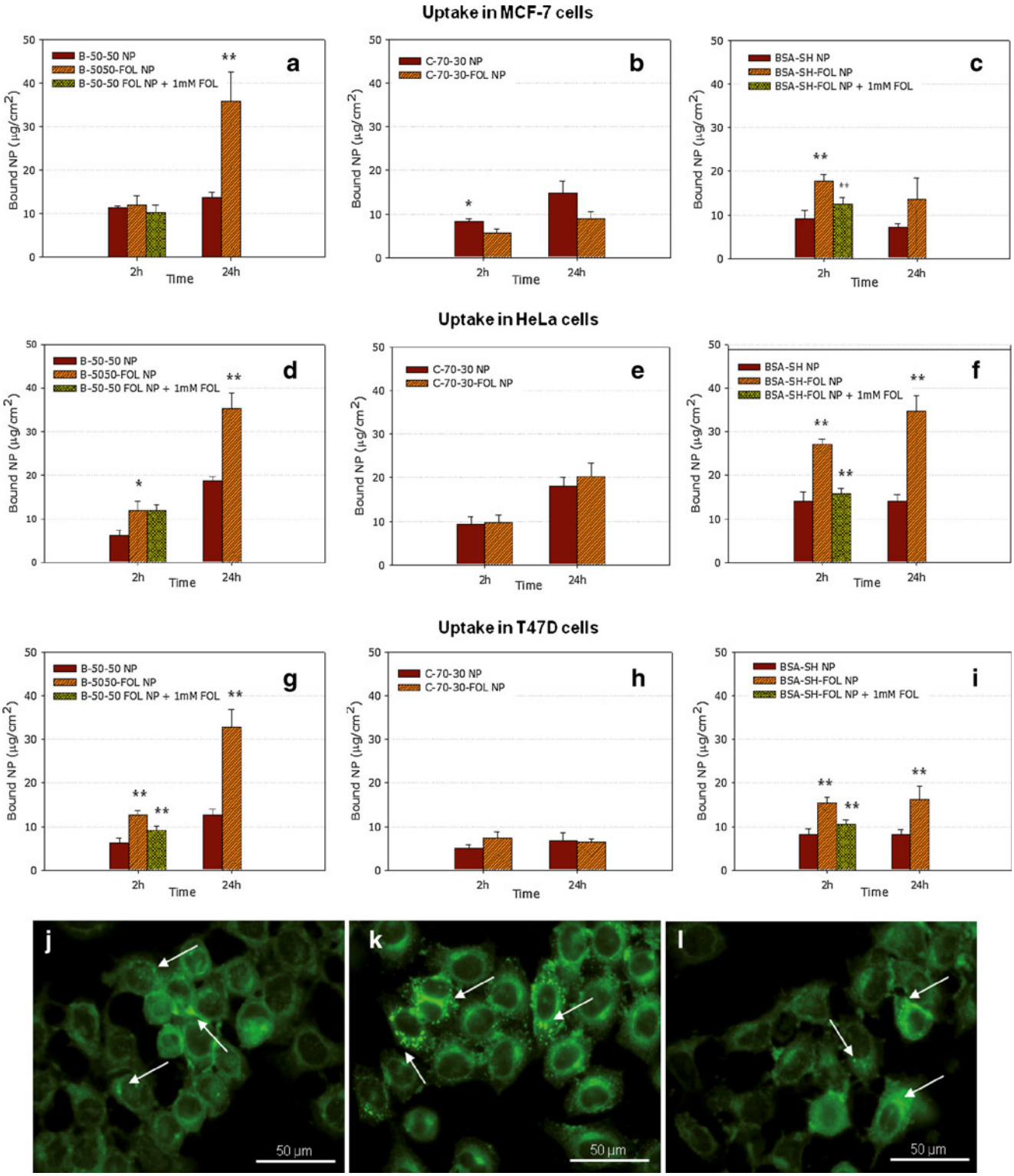

Fig. 4 Quantitative comparison of Coumarin-loaded internalized nanoparticles into MCF-7 (**a**, **b** and **c**), HeLa (**d**, **e** and **f**) and T47D cells (**g**, **h** and **i**). Fluorescence microscopy images of Coumarin-loaded BSA-SH-FOL NP in MCF-7 cells (**j**), Coumarin-loaded B-50-50-FOL NP in HeLa cells (**k**) and Coumarin-loaded C-70-30-FOL NP in T47D cells (**l**). *White arrows* indicate representative uptaken nanoparticles. Data marked with (*) showed significant differences ($p < 0.05$) and with (**) showed very significant differences ($p < 0.01$).

off-site toxicity and enhance efficacy against tumour cells. Previous works (14,15) showed good *in vitro* efficacy of TMX-loaded nanoparticles based on various mixtures of modified alginate and albumin as controlled drug delivery

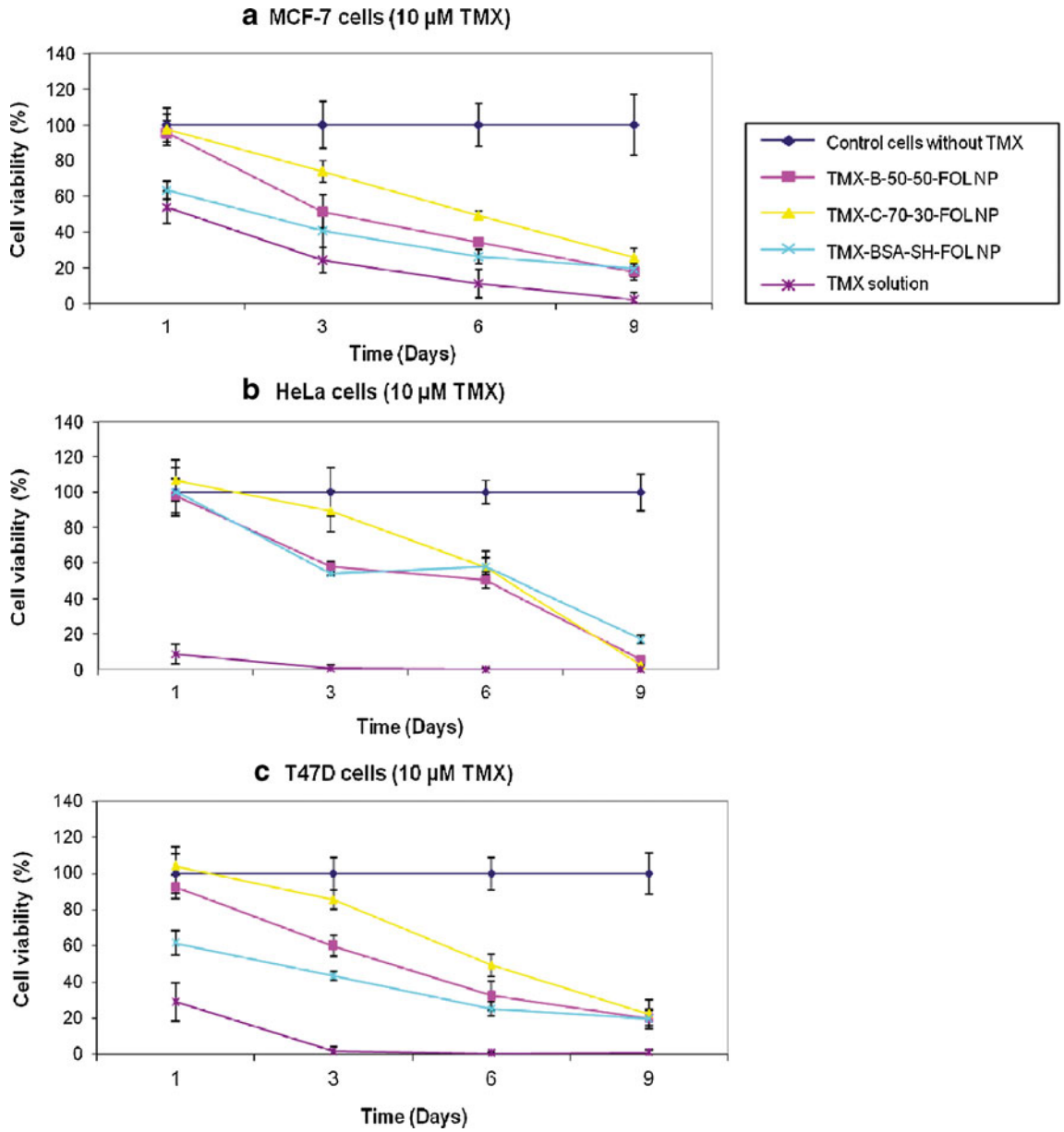

Fig. 5 Cell viability of MCF-7 (**a**), HeLa (**b**) and T47D (**c**) cells in presence of 10 μM TMX: without drug (—◆—); TMX solution (—✱—); TMX-BSA-SH-FOL (—×—); TMX-B-50-50-FOL (—■—) and TMX-C-70-30-FOL (—▲—).

systems. Additionally, an improved *in vivo* antitumor activity of TMX was declared after subcutaneous administration of these TMX-loaded nanoparticles in a breast tumour xenograft model (27). Consequently, the attachment of folic acid to these systems already tested could possible make an improvement of the effectiveness of TMX, and also in the development of new administration routes for this drug, such as intravenously.

Covalent attachment of folic acid to the three systems was successfully achieved. A very similar amount of folate content to that reported by Zhang and co-workers, who used the same methodology for BSA nanoparticles (18), was obtained. It seemed that when the proportion of BSA into the composition was reduced, a lower value of folate content was obtained, this being significantly different in the case of C-70-30-FOL NP. Since folic acid attachment occurred via amine groups of BSA, a lower value was expected in the composition with a lesser proportion of BSA in its composition.

Particles were characterized in terms of mean size and surface charge. Particles of very small size (≤100 nm) were obtained in all cases according to SEM micrographs. Quasi-elastic light scattering analysis confirmed this small size in the case of nanoparticles based on alginate/albumin mixtures. However, albumin nanoparticles showed a higher mean size value by this technique than deduced from the SEM micrographs. This difference could be explained in terms of nanoparticle aggregation phenomenon. Either unloaded or TMX-

loaded nanoparticles presented zeta potential values significantly lower than ±30 mV, which has been established as the minimum to obtain a physically stable nanosuspension and avoid nanoparticle aggregation (28). Thus, BSA-SH-FOL NP aggregates could be formed in aqueous medium, resulting in an increased mean size value when quasi-elastic study was performed. In the case of B-50-50-FOL and C-7030-FOL NP, zeta potential values were close to ±30 mV, resulting in stable nanosuspensions with similar mean size values by both techniques. Negative zeta potential values were obtained for unloaded formulations. This fact was expected due to the presence of BSA and alginate in nanoparticle composition, as other works have revealed (29,30). When nanoparticles were loaded with TMX, zeta potential values became positive in all cases. This fact could be attributed to the major superficial localization of the drug (31), according to the similar tendency observed in previous works (14,22).

TMX-load of nanoparticles was determined after tryptic hydrolysis of the systems. Results were very similar to those reported in previous studies (14), indicating that folate attachment did not affect TMX incorporation. Results of TMX extraction with methanol demonstrated again the superficial presence of TMX, as zeta potential values indicated. In the case of TMX-B-50-50-FOL and TMX-C-70-30-FOL NP, TMX extraction was complete; but in the case of TMX-BSA-SH-FOL NP, 62% of the drug was still trapped in the system. This fact was attributed to the strong interaction that can be established between TMX and the hydrophobic regions of albumin, as previous studies revealed (32). Superficial presence of the drug was additionally supported by fast TMX release during the first step of the release study performed with SDS, which is characteristic of hydrophobic drugs with this location (22). After this stage strongly retained TMX was released. Complete release of TMX was achieved within the first 24 h from all systems when SDS was included in the release medium. However, SDS would contribute to this fast and complete release, as previous studies showed (33). In fact, when a TMX release study was performed in PBS without SDS, the amount of drug released from the systems at 24 h diminished to 3–5% of total TMX load. SDS is a surfactant that is not present in physiological conditions. Consequently, if these nanoparticles were intravenously administered, almost all the loaded drug would remain intact and would be only released after the enzymatic digestion of nanoparticles, which would mainly occur after their cellular internalization. The presence of albumin into nanoparticle composition became a determinant factor for the release control (14,15). As a matter of fact, those compositions with a higher amount of albumin showed lower percentages of drug released in the first stage. Additionally, maximum drug release in these compositions was obtained later than in TMX-C-70-30-FOL.

Different cellular lines were used to test folate-targeted systems according to their expression of ER and FR. HeLa and T47D cells have been described in the literature as ER(−)&FR(+) and ER(+)&FR(+), respectively (34,35). MCF-7 cells have been described as positive in the expression of ER (35), but controversy has arisen in the case of folate receptor expression. Some authors have described this line as deprived in FR and, indeed, they used this line as negative control (36). However, there are works that describe them as weakly FR expressive (34) or even positive in the expression of FR receptor (37). Taking into account this controversial aspect, an immunofluorescence analysis was carried out in order to determine the FR expression level of each cell line. Results showed that all lines were positive in the expression of FR, especially HeLa cells, allowing these three lines to be used as possible *in vitro* test of folate-targeted system efficacy.

In general, good cytocompatibility values were obtained with B-50-50-FOL and C-70-30-FOL NP. This is in accordance with results previously obtained using non targeted systems (14). However, BSA-SH-FOL NP showed lower values of cell viability in the three lines than non targeted formulations (80%–100%) (14), indicating that this composition itself was relatively toxic. Since FR was determined in uptake studies as the main mechanism used by cells to internalize BSA-SH-FOL NP, only cells with FR over-expression, such as cancer cells, would be principally affected by this toxicity. Thus, BSA-SH-FOL NP itself would have a synergic antitumor action with TMX when loaded with this drug. In the case of B-50-50-FOL NP, uptake results could not clearly point to FR as the only mechanism of internalization, with the exception of T47D cells. This fact might indicate the existence of an unspecified mechanism that would act additionally to FR-mediated internalization. Thus, the presence of free folic acid in the incubation medium would not be sufficient to inhibit the internalization of the system. Previous works detected the presence of this unspecific uptake mechanism in MCF-7 and HeLa cells due to the presence of alginate in nanoparticle composition (14). Some authors revealed that negative-charged nanoparticles showed high cellular uptake levels due to electrostatic interactions established with some parts of cellular membrane (38,39). B-50-50-FOL NP showed more negative zeta potential values than BSA-SH-FOL NP and consequently, this system could only interact directly with cells due to its anionic surface, and this aspect creates difficulty in identifying the internalization via FR by this methodology. However, folic acid attachment to the systems, either in B-50-50-FOL or BSA-SH-FOL NP, led to a great enhancement of the nanoparticle uptake in all cellular lines. Consequently, FR-mediated uptake might be implicated in the internalization of both systems despite the fact that significant evidence was only found in BSA-SH-FOL NP. In the case of C-70-30-FOL NP, the amount of folate attached to the system was not enough to enhance its uptake. It seemed that an unspecific mechanism had a predominant role in this composition, which in fact showed the most negative zeta potential value.

When TMX was loaded into the systems, a gradual decrease in cell viability values was observed when TMX was being released from the all the systems. TMX-BSA-SH-FOL and TMX-B-50-50-FOL NP were especially effective in reducing cell viability from the third day of incubation. The amount of TMX that would be available within the cells treated with TMX-loaded systems would be lower than the amount of drug available in cells treated with TMX solution at 24 h, considering the amount of NP bound to cells at 24 h in uptake studies. However, folate-targeted systems may enter cells via folate receptor mediated endocytosis pathway ($Ka \sim 5 \times 10^{10}$ M for folate) (40), where much of the material is released into the cell cytoplasm after endocytosis and vesicular trafficking, and unligate folate receptor may then recycle to the cell surface. Since the recycling rate for the folate receptor is in the range of 0.5 to 5 h (41), more NP are expected to be introduced into the cells over 9 days. Moreover, folate conjugates have been observed to remain stable and functional for several hours following uptake by cancer cells (42), and TMX would be released only after NP degradation. This would justify the delayed cytotoxic action of folate targeted NP compared to TMX solution effect. Thus, the efficacy of TMX-FOL NP as a controlled drug release systems was demonstrated *in vitro*, where the systems with high folate content were the most effective against tumour cell survival.

In conclusion, this study demonstrates the promising *in vitro* anticancer action of these new TMX-loaded folate-targeted systems, especially TMX-BSA-SH-FOL and TMX-B-50-50 NP-FOL, which showed the highest cell uptake values and effectiveness in reducing carcinoma cell survival. TMX incorporation to these folate-targeted systems may allow a new administration route to be studied in further *in vivo* studies in order to improve current TMX therapy.

ACKNOWLEDGMENTS AND DISCLOSURES

Authors are grateful to Dr. Von Kobbe, Dr. Tierrez and Dr. Perez-Castillo for the gift of MCF-7, HeLa and T47D cells, respectively. The financial support of the Ministerio de Ciencia e Innovación of Spain (FIS PS09/01513 and MAT2010-21509-C03-03) and the FPI grant to A. Martínez are gratefully acknowledged.

REFERENCES

1. Bray F, Jemal A, Grey N, Ferlay J, Forman D. Global cancer transitions according to the Human Development Index (2008–2030): a population-based study. Lancet Oncol. 2012;13(8):790–801.
2. Moghimi SM, Hunter AC, Murray JC. Nanomedicine: current status and future prospects. FASEB J. 2005;19(3):311–30.
3. Park JH, von Maltzahn G, Xu MJ, Fogal V, Kotamraju VR, Ruoslahti E, et al. Cooperative nanomaterial system to sensitize, target, and treat tumors. Proc Natl Acad Sci U S A. 2010;107(3):981–6.
4. Davis ME, Chen ZG, Shin DM. Nanoparticle therapeutics: an emerging treatment modality for cancer. Nat Rev Drug Discov. 2008;7(9):771–82.
5. Ranganathan R, Madanmohan S, Kesavan A, Baskar G, Krishnamoorthy YR, Santosham R, et al. Nanomedicine: towards development of patient-friendly drug-delivery systems for oncological applications. Int J Nanomed. 2012;7:1043–60.
6. Puri A, Loomis K, Smith B, Lee JH, Yavlovich A, Heldman E, *et al.* Lipid-based nanoparticles as pharmaceutical drug carriers: from concepts to clinic. Crit Rev Ther Drug Carr Syst. 2009;26(6):523–80.
7. Sudimack J, Lee RJ. Targeted drug delivery via the folate receptor. Adv Drug Deliv Rev. 2000;41(2):147–62.
8. Xia W, Low PS. Folate-targeted therapies for cancer. J Med Chem. 2010;53(19):6811–24.
9. Ulbrich K, Michaelis M, Rothweiler F, Knobloch T, Sithisarn P, Cinatl J, et al. Interaction of folate-conjugated human serum albumin (HSA) nanoparticles with tumour cells. Int J Pharm. 2011;406(1–2):128–34.
10. Yang SJ, Lin FH, Tsai HM, Lin CF, Chin HC, Wong JM, *et al.* Alginate-folic acid-modified chitosan nanoparticles for photodynamic detection of intestinal neoplasms. Biomaterials. 2011;32(8):2174–82.
11. Benichou A, Aserin A, Garti N. Protein-Polysaccharide Interactions for Stabilization of Food Emulsions. J Dispers Sci Technol. 2002;23(1–3):93–123.
12. Yi YM, Yang TY, Pan WM. Preparation and distribution of 5-fluorouracil (125)I sodium alginate-bovine serum albumin nanoparticles. World J Gastroenterol. 1999;5(1):57–60.
13. Ameller T, Legrand P, Marsaud V, Renoir JM. Drug delivery systems for oestrogenic hormones and antagonists: the need for selective targeting in estradiol-dependent cancers. J Steroid Biochem Mol Biol. 2004;92(1–2):1–18.
14. Martinez A, Benito-Miguel M, Iglesias I, Teijon JM, Blanco MD. Tamoxifen-loaded thiolated alginate-albumin nanoparticles as antitumoral drug delivery systems. J Biomed Mater Res A. 2012;100A(6):1467–76.
15. Martínez A, Iglesias I, Lozano R, Teijón JM, Blanco MD. Synthesis and characterization of thiolated alginate-albumin nanoparticles stabilized by disulfide bonds. Evaluation as drug delivery systems. Carbohydr Polym. 2011;83(3):1311–21.
16. Bernkop-Schnurch A. Thiomers: a new generation of mucoadhesive polymers. Adv Drug Deliv Rev. 2005;57(11):1569–82.
17. Lee RJ, Low PS. Delivery of liposomes into cultured KB cells via folate receptor-mediated endocytosis. J Biol Chem. 1994;269(5):3198–204.
18. Zhang L, Hou S, Mao S, Wei D, Song X, Lu Y. Uptake of folate-conjugated albumin nanoparticles to the SKOV3 cells. Int J Pharm. 2004;287(1–2):155–62.
19. Lee KH, Ward BA, Desta Z, Flockhart DA, Jones DR. Quantification of tamoxifen and three metabolites in plasma by high-performance liquid chromatography with fluorescence detection: application to a clinical trial. J Chromatogr B Anal Technol Biomed Life Sci. 2003;791(1–2):245–53.
20. MacCallum J, Cummings J, Dixon JM, Miller WR. Solid-phase extraction and high-performance liquid chromatographic determination of tamoxifen and its major metabolites in plasma. J Chromatogr B Biomed Appl. 1996;678(2):317–23.
21. Hu FX, Neoh KG, Kang ET. Synthesis and in vitro anti-cancer evaluation of tamoxifen-loaded magnetite/PLLA composite nanoparticles. Biomaterials. 2006;27(33):5725–33.
22. Chawla JS, Amiji MM. Biodegradable poly(epsilon -caprolactone) nanoparticles for tumor-targeted delivery of tamoxifen. Int J Pharm. 2002;249(1–2):127–38.
23. Beerli RR, Dreier B, Barbas 3rd CF. Positive and negative regulation of endogenous genes by designed transcription factors. Proc Natl Acad Sci U S A. 2000;97(4):1495–500.

24. Corona G, Giannini F, Fabris M, Toffoli G, Boiocchi M. Role of folate receptor and reduced folate carrier in the transport of 5-methyltetrahydrofolic acid in human ovarian carcinoma cells. Int J Cancer. 1998;75(1):125–33.
25. Shi G, Guo W, Stephenson SM, Lee RJ. Efficient intracellular drug and gene delivery using folate receptor-targeted pH-sensitive liposomes composed of cationic/anionic lipid combinations. J Control Release. 2002;80(1–3):309–19.
26. Han X, Liu J, Liu M, Xie C, Zhan C, Gu B, et al. 9-NC-loaded folate-conjugated polymer micelles as tumor targeted drug delivery system: preparation and evaluation in vitro. Int J Pharm. 2009;372(1–2):125–31.
27. Martinez A, Muniz E, Iglesias I, Teijon JM, Blanco MD. Enhanced preclinical efficacy of tamoxifen developed as alginate-cysteine/disulfide bond reduced albumin nanoparticles. Int J Pharm. 2012;436(1–2):574–81.
28. Muller RH, Jacobs C, Kayser O. Nanosuspensions as particulate drug formulations in therapy. Rationale for development and what we can expect for the future. Adv Drug Deliv Rev. 2001;47(1):3–19.
29. Arnedo A, Espuelas S, Irache JM. Albumin nanoparticles as carriers for a phosphodiester oligonucleotide. Int J Pharm. 2002;244(1–2):59–72.
30. Aynie I, Vauthier C, Chacun H, Fattal E, Couvreur P. Spongelike alginate nanoparticles as a new potential system for the delivery of antisense oligonucleotides. Antisense Nucleic Acid Drug Dev. 1999;9(3):301–12.
31. Abbasalipurkabir R, Salehzadeh A, Abdullah R. Delivering Tamoxifen within Solid Lipid Nanoparticles. Pharm Technol. 2011;35(4):74–9.
32. Morello KC, Wurz GT, DeGregorio MW. Pharmacokinetics of selective estrogen receptor modulators. Clin Pharmacokinet. 2003;42(4):361–72.
33. Martinez A, Arana P, Fernández A, Olmo R, Teijón C, Blanco MD. Synthesis and characterisation of alginate/chitosan nanoparticles as tamoxifen controlled delivery systems. Journal of Microencapsulation.
34. Geszke M, Murias M, Balan L, Medjahdi G, Korczynski J, Moritz M, et al. Folic acid-conjugated core/shell ZnS:Mn/ZnS quantum dots as targeted probes for two photon fluorescence imaging of cancer cells. Acta Biomater. 2011;7(3):1327–38.
35. Walter P, Green S, Greene G, Krust A, Bornert JM, Jeltsch JM, et al. Cloning of the human estrogen receptor cDNA. Proc Natl Acad Sci U S A. 1985;82(23):7889–93.
36. Sonvico F, Mornet S, Vasseur S, Dubernet C, Jaillard D, Degrouard J, et al. Folate-conjugated iron oxide nanoparticles for solid tumor targeting as potential specific magnetic hyperthermia mediators: synthesis, physicochemical characterization, and in vitro experiments. Bioconjug Chem. 2005;16(5):1181–8.
37. Suzuki T, Hisakawa S, Itoh Y, Suzuki N, Takahashi K, Kawahata M, et al. Design, synthesis, and biological activity of folate receptor-targeted prodrugs of thiolate histone deacetylase inhibitors. Bioorg Med Chem Lett. 2007;17(15):4208–12.
38. Wilhelm C, Gazeau F, Roger J, Pons JN, Bacri JC. Interaction of Anionic Superparamagnetic Nanoparticles with Cells: Kinetic Analyses of Membrane Adsorption and Subsequent Internalization. Langmuir. 2002;18(21):8148–55.
39. Wilhelm C, Billotey C, Roger J, Pons JN, Bacri JC, Gazeau F. Intracellular uptake of anionic superparamagnetic nanoparticles as a function of their surface coating. Biomaterials. 2003;24(6):1001–11.
40. Jansen G. Receptor-, and carrier-mediated transport systems for folates, and antifolates. In: Jackman AL, editor. Antifolate drugs in cancer therapy. Totowa: Humana Press; 1999. p. 293–321.
41. Ke CY, Mathias CJ, Green MA. The folate receptor as a molecular target for tumor-selective radionuclide delivery. Nucl Med Biol. 2003;30(8):811–7.
42. Leamon CP, Low PS. Delivery of macromolecules into living cells: a method that exploits folate receptor endocytosis. Proc Natl Acad Sci U S A. 1991;88(13):5572–6.